Microchimica Acta (2020) 187:266
https://doi.org/10.1007/s00604-020-4218-7

ORIGINAL PAPER

Electrochemical determination of zearalenone using a label-free competitive aptasensor

Farah Asilah Azri[1] · Shimaa Eissa[2] · Mohammed Zourob[2] · Raja Chinnappan[2] · Rashidah Sukor[1,3] · Nor Azah Yusof[4] · Nurul Hanun Ahmad Raston[5] · Ali Alhoshani[6] · Selamat Jinap[1,3]

Received: 23 October 2019 / Accepted: 6 March 2020

Abstract

An electrochemical aptasensor is described for determination of the phytohormone of zearalenone (ZEA). The gold electrode was modified with ZEA via covalent attachment using cysteamine-hydrochloride and 1,4-phenylene diisocyanate linker. A truncated ZEA aptamer with a dissociation constant of 13.4 ± 2.1 nM was used in an aptasensor. The electrochemical property was investigated using square wave voltammetry for monitoring the change in the electron transfer using the ferro/ferricyanide system as redox probe. Under optimal experimental conditions, the response was best measured at a potential of 0.20 V (vs. Ag/AgCl). The signals depended on the competitive mechanism between the immobilised ZEA and free ZEA for the aptamer binding site. The aptasensor works in the range 0.01 to 1000 ng·mL^{-1} ZEA concentration, with a detection limit of 0.017 ng·mL^{-1}. High degree of cross-reactivity with the other analogues of ZEA was observed, whereas none towards other mycotoxins. The aptasensor was further applied for the determination of ZEA in the extract of maize grain and showed good recovery percentages between 87 and 110%.

Keywords Biosensor · Zearalenone · Aptamer · Square wave voltammetry · Electrochemical impedance spectroscopy

Introduction

Zearalenone (ZEA) is an oestrogenic mycotoxin produced by several *Fusarium* species (e.g., *F. graminearium, F. culmorum, F. cerealis, F. equiseti, F. crookwellense, and F. semitectum*). Zearalenone commonly contaminates cereal crops including maize, barley oats, wheat, rice and sorghum. The production of ZEA is not only taking place during pre-harvest stage but also arises during post-harvest. It occurs when the crops are not properly managed under suitable conditions [1]. ZEA and its hydroxylated derivatives such as α- and β-zearalenol (α-ZEL, β-ZEL) are resorcyclic acid lactone (non-steroidal). They can cause strong oestrogenic effects and reproductive toxicity (TDI 0.25 μg kg^{-1} body weight) [2]. The toxic effects of ZEA and its metabolites primarily derived from their oestrogenic properties. This is because they can mimic a structural shape of the natural occurring oestrogens, oestradiol, oestrone and oestriol which interacts with human oestrogen receptors [3]. They have a very high relative binding affinity for both oestrogen receptor ER-B and high

Electronic supplementary material The online version of this article (https://doi.org/10.1007/s00604-020-4218-7) contains supplementary material, which is available to authorized users.

✉ Selamat Jinap
sjinap@gmail.com; jinap@upm.edu.my

[1] Food Safety and Food Integrity, Institute of Tropical Agriculture and Food Security, Universiti Putra Malaysia, 43400 UPM Serdang, Selangor, Malaysia

[2] Department of Chemistry, Alfaisal University, Al Zahrawi Street, Al Maather, AlTakhassusi, Riyadh 11533, Saudi Arabia

[3] Department of Food Science, Faculty of Food Science and Technology, Universiti Putra Malaysia, 43400 UPM Serdang, Selangor, Malaysia

[4] Department of Chemistry, Faculty of Science, Universiti Putra Malaysia, 43400 UPM Serdang, Selangor, Malaysia

[5] School of Bioscience and Biotechnology, Faculty of Science and Technology, Universiti Kebangsaan Malaysia, 43600 Bangi, Selangor, Malaysia

[6] Department of Pharmacology and Toxicology, College of Pharmacy, King Saud University, Riyadh 11533, Saudi Arabia

Published online: 12 April 2020

transactivation activity [4]. Hyperoestrogenic syndromes can cause early sexual maturity, prolapse of the vagina or rectum, miscarriage, underdeveloped embryos, uterine enlargement, swelling of the valve, mammary glands and nipples, prolonged or interrupted oestrus and pseudopregnancy [5]. Besides, ZEA may cause changes in the reproductive tract of the animals especially mice, rats, guinea pigs, rabbits, cattle and poultry with pigs as the most sensitive animals [6].

Conventionally, quantitative chromatographic and immunologic assays such as ELISA are commonly used to detect these low molecular weight mycotoxins in agriculture commodities [7]. Although these analytical methods provide precision, accuracy, sensitivity and reproducibility, they are not applicable for on-site analysis. This is because, they require extensive sample preparation, expensive equipment, skilled operators and may lack accuracy at low analyte concentration [8]. Therefore, biosensors appeared as advanced tools offering some advanced features including simplicity, easy-to-use, relatively fast and portability [9]. Previously, the voltammetric behaviour of ZEA was studied using cyclic voltammetry (CV), differential pulse voltammetry (DPV), and electrochemical impedance spectroscopy (EIS) [10]. This determination technique requires no biorecognition elements as it measures the adsorptive behaviour and oxidation process of the ZEA on the electrode. Furthermore, some immunosensors have been reported for the determination of ZEA, incorporating various platforms and modifications [11–14]. Although immunosensors are ideal methods for detecting mycotoxins without extensive cleanup, the use of antibodies in these methods are generally expensive. Furthermore, it requires strict physiological conditions as they are sensitive to temperature. The production of antibodies also requires animals or cell cultures which are time-consuming and costly. It is important to explore the application of the new biorecognition molecule for ZEA which is aptamers that are easier to produce with good reproducibility and higher stability [15].

Aptamers are the trending alternatives of antibodies in biosensor development especially for the determination of low molecular weight molecules such as toxins, antibiotics, drugs, heavy metals and ions [16]. Aptamers are single-stranded, synthetic oligonucleotides (DNA or RNA) that are able to fold into 3-dimensional shapes. It can bind non-covalently to the target molecule with high affinity [16]. Aptamers have been extensively used in diagnosis, detection and chemical analysis of various substances. These are due to their inherent specificity and affinity. Systematic evolution of ligands by exponential enrichment (SELEX) is a well-established in vitro method for aptamers selection. This method consists of a few steps, mainly binding, partitioning and amplification [17]. Once the aptamer sequence is recognized, it can be reproducibly synthesised with high purity [18]. This permits inexpensive and rapid production and with high consistency from each batch [19].

An aptamer recognising ZEA was selected by Chen et al. [15] after 14 rounds of SELEX using magnetic beads. This aptamer has been further utilized in the development of a few biosensors based on various techniques including fluorescence [20–22], colorimetric [23, 24], lateral flow [25] and electrochemical [26]. However, these sensors still require labelling of the bioreceptors which increase the cost of the overall assay and are mostly semi-quantitative. Electrochemical biosensors offer several advantages in terms of high sensitivity, low cost and capability of employing label-free format and miniaturization. Herein, a label-free indirect competitive electrochemical aptasensor was reported for the determination of ZEA. Chen et al. [15] have reported the best ZEA aptamer ($8Z_{31}$) with a dissociation constant (K_d) of 41 ± 5 nM. The same aptamer was truncated in this study by eliminating the primer-binding sites of the original sequence and subsequently increase the aptamers affinities.

The main challenge of detecting small molecules using aptasensors is usually related to the small conformational changes occurring within the aptamer upon aptamer-target binding. The conformational changes usually lead to small signal changes in direct binding assays. Therefore, indirect competitive format was employed by immobilising the ZEA onto the gold electrode using cysteamine-hydrochloride (Cys-HCl) and 1,4-phenylene diisocyanate (PDIC) linker. The free ZEA in the sample was allowed to compete with the immobilised ZEA for the binding site of fixed amount ZEA aptamer.

Experimental

Reagents, materials and instrumentation

All reagents, materials and instrumentation used in this work are described in detail in the Electronic Supplementary Material (ESM).

Immobilisation of the zearalenone onto the gold electrode surface

The immobilisation protocol was done according to Eissa et al. [27] with minor modifications. The gold electrode (2 mm in diameter) was polished using alumina slurries (Al_2O_3), followed by washing with Milli-Q water and ethanol. The electrode was then sonicated for 10 min. Gold cleaning was done using cyclic voltammetry (CV) after treatment with piranha solution (H_2S0_4:H_2O_2, 3:1) for 2 min. The electrode was cleaned electrochemically in 0.1 M H_2SO_4 for 5 min with a scan rate of 100 mV s^{-1}, at potential range of − 0.2 and 1.6 V for 30 cycles. The cleaned and pre-treated electrode was then immersed for 2 h in freshly prepared 10 mM of Cys-HCl in ultrapure water. The electrode was then washed using ethanol

for 1–2 times to remove the excess Cys-HCl. Next, the Au/Cys electrode was incubated in 6.5 mM of PDIC solution in toluene for another 2 h to activate the terminal amine groups of the Cys. The Au/Cys/PDIC electrode was rinsed again twice using DMF. Twenty microliters of 100 μg·mL^{-1} ZEA solution in ACN was placed onto the top of the gold electrode surface and incubated for another 2 h at room temperature. The Au/Cys/PDIC/ZEA electrode was then washed excessively with ACN to remove the unbound ZEA. Finally, the electrode was incubated in MeOH overnight to block the remaining free isocyanate groups. The immobilised electrodes were stored at 4 °C until further used.

Electrochemical measurements

The EIS measurements were done over a frequency range from 10 kHz to 1.0 Hz by means of an alternative voltage with amplitude of 10 mV, superimposed on a DC potential of 0.20 V (vs. Ag/AgCl reference electrode). The square wave voltammetry (SWV) measurements were performed over a potential range from 0.45 to 0.1 V at a scan rate of 0.125 V s^{-1}, with 0.02 V amplitude and a frequency of 25 Hz. All measurements were conducted in the redox solution.

Determination of the dissociation constant by electrochemical impedance spectroscopy

The affinity of the truncated aptamer towards ZEA was determined by performing electrochemical binding assay using a constant amount of ZEA immobilised on the electrode and different concentrations of the aptamer (0 to 250 nM). The immobilisation of ZEA on the electrode was done as described previously. The measurements were performed by electrochemical impedance spectroscopy (EIS) to monitor the charge transfer resistance (R_{CT}). The saturation curve was attained, and the dissociation constant (K_d) for the ZEA aptamer was evaluated by non-linear regression analysis using GraphPad Prism 5 software.

Characterisation of the conformational change of the ZEA aptamer

Circular dichroism (CD) spectroscopy was used to observe the conformational change of the aptamer in the presence of the analyte. The analysis was performed using 1.0 μM ZEA aptamer in binding buffer, pH 7.4. The measurements were done using quartz cuvette in an optical chamber with a 0.1 cm path length. The chamber was purged with dry purified nitrogen gas (99.99%) prior to use and was kept in the nitrogen atmosphere along the measurements. Each CD spectrum was scanned from 340 to 230 nm at 0.1 nm intervals, accumulation of three scans at 50 nm min^{-1} with a 1 nm band width and time constant of 1 s.

Optimisation of the experimental conditions of the aptasensor

Several experimental conditions were optimised to obtain the maximum performance of the aptasensor including concentration of aptamer, binding time and pH of the binding buffer. The concentration of the aptamer was tested in the range of 0 to 100 nM with a constant concentration of ZEA (100 μg·mL^{-1}) immobilised on the electrode. The binding of aptamer and ZEA was evaluated at various time intervals from 5 to 70 min. Different pH of binding buffer (pH 3, 5, 7, 7.4, 9 and 11) was used to determine the optimum pH for the aptamer-toxin binding. The binding was monitored by measuring the change in the reduction current using SWV in ferro/ferricyanide redox solution as described above.

Electrochemical competitive assay

The zearalenone detection assay, cross-reactivity and testing in real sample were done as follows: the aptamer was first pretreated by heating at 90 °C for 5 min, followed by 5 min at 4 °C and 10 min at room temperature. Then, 10 μL of the specific concentrations (0.001 to 1000 ng·mL^{-1}) of free ZEA was pre-incubated with 50 nM of ZEA aptamer for 10 min at room temperature. The mixture was then transferred onto the immobilised Au/Cys/PDIC/ZEA electrode and further incubated for 35 min. The electrode was then washed with 0.1 M Tris buffer before proceed with the measurement using SWV in the redox couple. The binding capacity was then evaluated by calculating the percentage of reduction current signal change, after considering the background signal.

Extraction of maize grain sample

Preparation of the maize grain sample was performed according to Shim et al. [28]. The maize grain sample was collected from silo at maize plantation field in Terengganu, Malaysia. The sample was first ground using blender to obtain the maize powder. Then, the maize powder was spiked with 0.1, 1 and 10 ng·mL^{-1} of ZEA. The spiked samples were kept at room temperature (25 °C) for 4 h in the dark to evaporate the acetonitrile in ZEA standards. The spiked powdered samples (1 g) were extracted using 3 mL of 20% methanol/water (*v*/v) for 15 min at room temperature and then centrifuged at 4000×*g* for 5 min at 4 °C. The supernatants were filtered through a disposable syringe filter (0.2 μm) and diluted tenfold with binding buffer to minimize matrix and methanol effects.

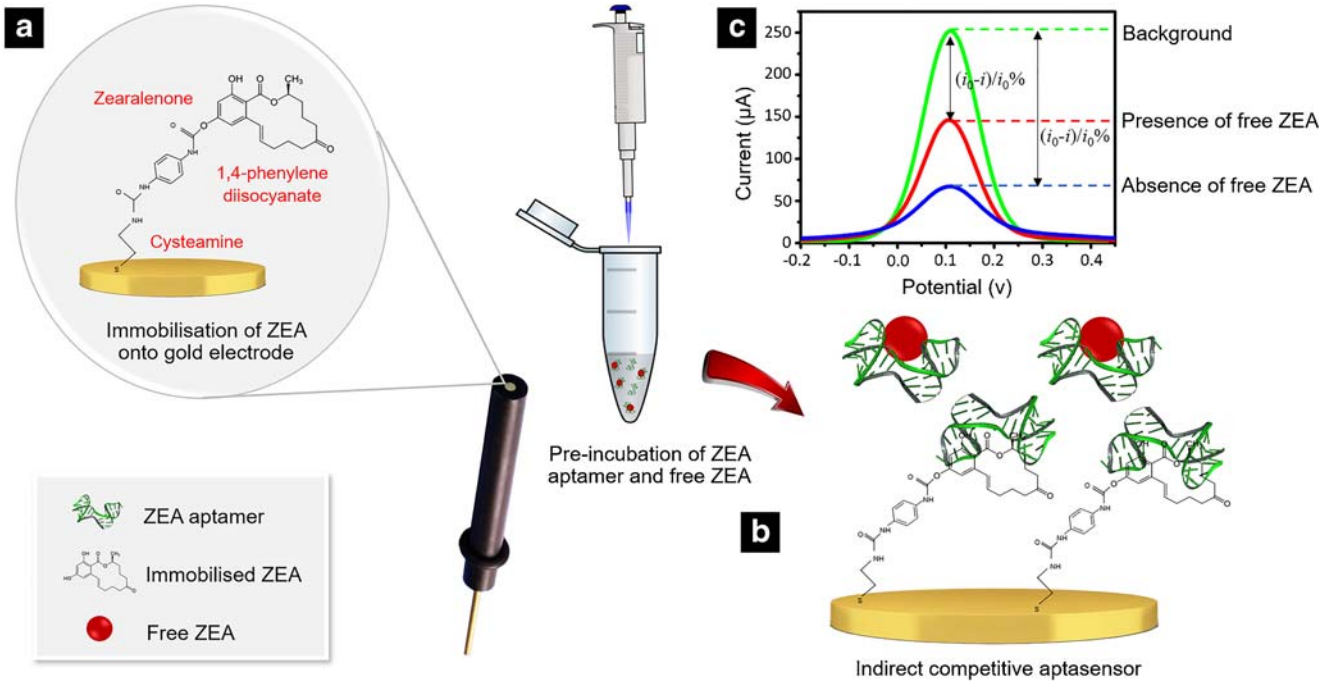

Fig. 1 Schematic representation of the electrochemical determination of zearalenone based on indirect competitive assay. Step **a** Immobilisation of ZEA on the surfaces of gold electrode via covalent attachment, **b** competition for the ZEA aptamer binding site between immobilised and free ZEA and **c** current signal of the binding event based on SWV technique

Results and discussion

Characterisation of the immobilisation steps of the ZEA on the electrodes

The ZEA molecules were immobilised onto the gold working electrode via its hydroxyl groups following the schematic shown in Fig. 1. SWV and EIS were used to ascertain the immobilisation of the ZEA onto the electrode. The SWV voltammograms and impedance Nyquist plots of the immobilisation procedure are provided in the Electronic Supplementary Material (Fig. S1). Increase in the reduction peak current can be observed after the surface of the Au electrode was functionalised with Cys. This increment was expected owing to the electrostatic attraction between the $[Fe(CN)_6]^{4-/3-}$ anions and the positively charged amine terminal groups of Cys [29]. However, after the incubation with the bifunctional linker, PDIC, the peak current decreased significantly indicating the attachment of the amine groups of the Cys. This is due to the negatively charged isocyanate groups which repel the redox anions from the surface [30]. After the immobilisation of the ZEA molecules, the current was further decreased which implies the blocking of the surface with ZEA molecules and subsequently lessen the electron transfer rate. It is also worth noting that the pKa of the diphenolic ZEA molecule is 7.62 which suggested that at the working pH of 7.4, the phenol anion exist in the solution [31]. This negative charge also repels the redox molecules and causes a decrease in the current. Methanol was used as the blocking agent to block the available active groups of the PDIC, and it was proven by observing increment in current peak right after the blocking step.

Charge transfer resistance (R_{CT}) was used as the main parameter in the EIS spectra. It represents the resistance towards the electron transfer process across the electrolyte interface. The semicircles at higher frequencies confirm the electron transfer-limited process, and the straight lines at lower frequencies indicate the diffusion process [27]. A straight line with a very small semicircle of the bare gold electrode indicates the electron transfer was very fast and the process is controlled by diffusion. After the addition of Cys, the R_{CT} value decreased from 271 to 11.5 Ω, and only a straight line was observed. This is due to the positive amine groups on the electrode (Au/Cys). The immobilisation of ZEA onto the electrode showed a significant increase in the R_{CT} value to 823 Ω due to the blocking behaviour of the ZEA [32]. The results obtained from both SWV and EIS measurements confirm the accomplishment of the ZEA molecule immobilisation onto the gold electrode surface.

Binding affinity analysis of the truncated aptamer

Previous study reported an 80-nt nucleotides ZEA aptamer sequence ($8Z_{31}$) as the optimum aptamer for ZEA with a dissociation constant (K_d) of 41 ± 5 nM [15]. However, in this study, the sequence was truncated by removing the primer binding sites. After the separation steps in SELEX, primer annealing sites are utilized for the

enzymatic amplification of the libraries. These primer sequences represent more than half of the aptamer sequence and consist of persistent sequences that interact non-specifically with the analyte of interest or minimise the complexity of the aptamer. This may be because the primers' sequences usually represent negligible binding motif and also have minimum structural function [33]. It is proven that generating minimal length of the aptamer by eliminating unnecessary nucleotides can increase the aptamers' affinities [34].

Therefore, the central 40-nt bases of the aptamer sequence were reproduced as new aptamer. It was necessary to evaluate the binding affinity of the shortened aptamer towards its target by electrochemical binding assay. A constant amount of ZEA was immobilised onto the electrode, and different concentrations of aptamer (ranging from 0 to 250 nM) were used to evaluate the K_d. The Nyquist plots in Fig. 2a show that the semicircles were gradually increased with the increasing concentration of the aptamer indicating the increment of R_{CT}. This is attributed to more binding of the aptamer to the ZEA on the electrode leading to higher negatively charged DNA shielded on the surface. As shown in Fig. 2b, the K_d was then calculated using non-linear regression analysis by plotting the percentage change of the R_{CT} [$(R-R_0)/R_0\%$] versus the aptamer concentration (nM). From the binding curve, the K_d of the truncated aptamer was calculated to be 13.4 ± 2.1 nM which is lower than the reported K_d [15] of full ZEA aptamer sequence. Hence, these results support that the ZEA aptamer can be preferably used without the primers regions.

Circular dichroism of the aptamer

The secondary structure predictions of the ZEA aptamer sequence with and without the primer regions are shown in Fig. 3a and b, respectively. Based on Fig. 3a, the structure of the aptamer was assembled from stems, loops and bulges. However, after eliminating the primer regions, the structure of the aptamer was predicted as hairpins. Basically, the binding of aptamers to their targets is based on structural compatibility, aromatic ring stacking, electrostatic, Van der Waals interaction and hydrogen bonding [35]. Based on Chen et al., TAT, TAC and CAT appeared recurrently in the sequences, and these regions might be the crucial elements of possible binding sites [15].

(5'-T**CAT**C**TAT**C**TAT**GG**TACATTACTAT**CTGT AATGTGA**TAT**G-3)

Circular dichroism (CD) measurements were carried out to determine the conformational changes of the aptamer that confirm the docking between ZEA and its aptamer. CD is usually used for molecules such as nucleic acids and proteins containing chiral atoms. It measures the differential absorption of left and right polarized light by the analytes [36]. The addition of ZEA produced a decrease in the positive elliptic maximum around 275 nm and right shift of the negative minimum around 255 nm (Fig. 3c). This result is in agreement with Chen et al. which showed a similar ligand-DNA interaction between ZEA and the 80-nt ZEA aptamer [15]. It shows that the 40-nt ZEA aptamer exhibits similar trend of conformational change on the secondary structure upon binding to ZEA. According to these results, the possibility of detecting the ZEA in a direct sensing format was tested by immobilizing the aptamer on the electrode (data not shown). However, minimal sensor response was obtained which indicated that the conformational changes within the aptamer sequence upon target binding were insufficient to be detected on the sensor surface.

Optimisation of the aptamer-ZEA binding conditions

In order to optimise the binding conditions for attaining the optimal detection sensitivity, the aptamer concentration,

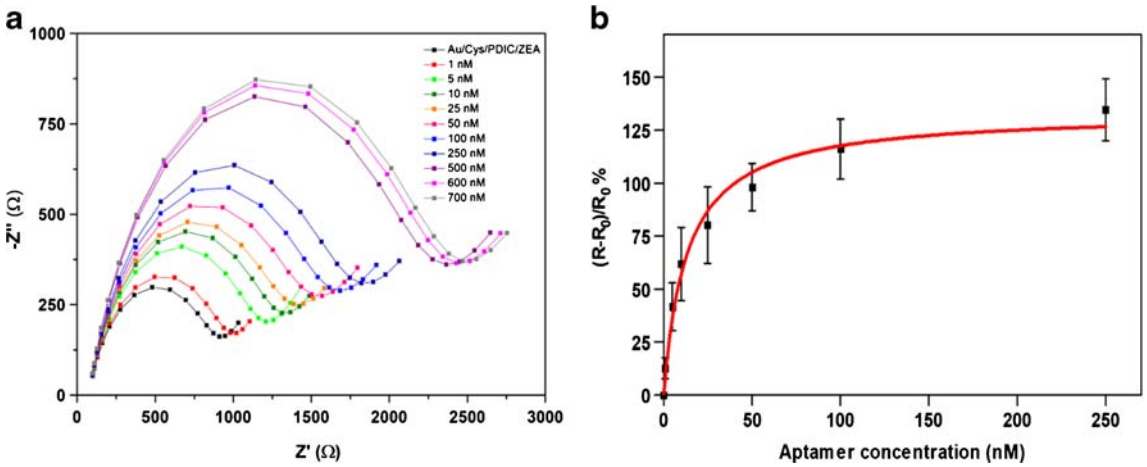

Fig. 2 **a** Nyquist plots of the ZEA electrode before and after incubation with different concentration of ZEA aptamer and **b** non-linear regression plot of $(R-R_0)/R_0\%$ signal vs. aptamer concentration (nM) with K_d of 13.4 ± 2.1 nM and R^2 of 0.986. The error bars represent the standard deviations of the measurements ($n = 2$)

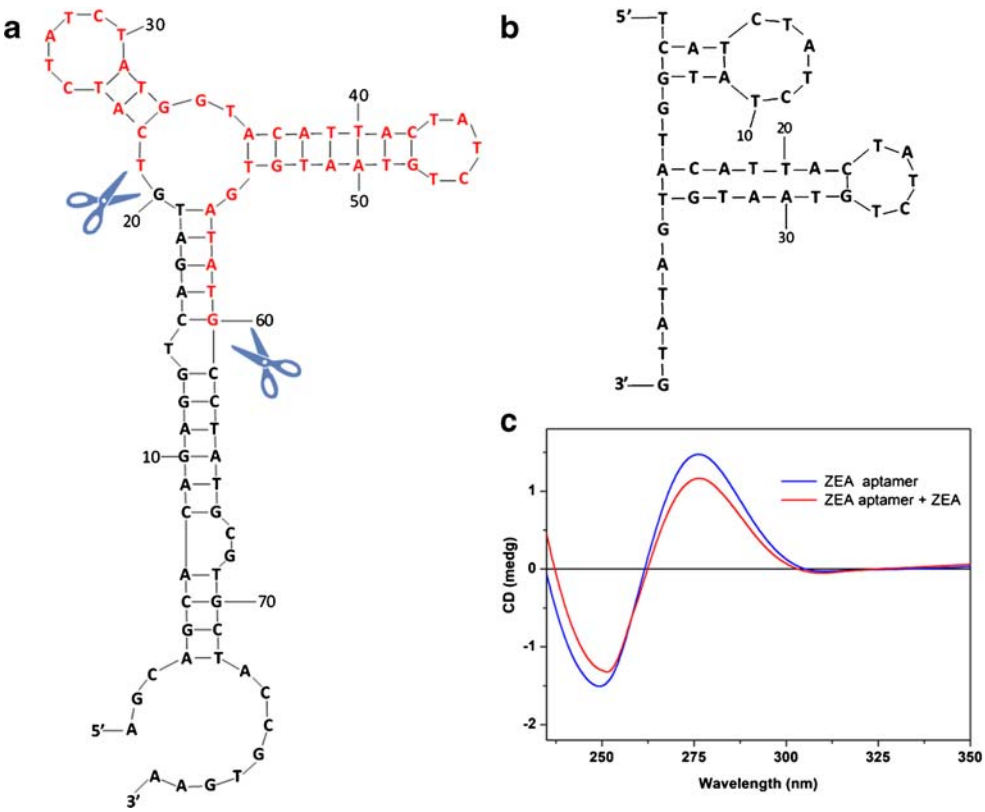

Fig. 3 **a** Secondary structure model of the ZEA aptamer with full sequence predicted by Mfold software. The bases in red represents the truncated middle random sequence without the primer sites, **b** Secondary structure model of truncated ZEA aptamer and **c** circular dichroism spectra of truncated ZEA aptamer in the presence of ZEA

incubation time and pH of the binding buffer were examined. Figure 4a shows the SWV signals for the modified electrodes before and after incubation with the aptamer. It is apparent that the reduction peak current is significantly decreased upon binding of the aptamer to the ZEA due to the negative charges of the aptamer which repel the redox anions. Figure 4b shows the $(i_0\text{-}i)/i_0\%$ signal of the ZEA electrode after incubation with different concentrations of ZEA aptamer. An enhancement in the signal is observed as the concentration of the aptamer was gradually increased to 50 nM at saturation point. In general, higher concentration of aptamer will lead to decrease in the sensitivity of the assay, and lower concentration will lead to small signal value [27]. Therefore, the 50-nM ZEA aptamer was chosen for the competitive assay to strike a balance between the two effects. Figure 4c displays the effect of pH of the binding buffer on the aptamer-analyte binding. It is shown that the binding of the aptamer was diminished at alkaline pHs (9 and 11). There is no significant effect on the binding at pH < 7.4. Following the routine incubation time, a few points from 5 to 70 min were investigated, and the result is displayed in Fig. 4d. Based on the result, $(i_0\text{-}i)/i_0\%$ signal increased with the increasing time. An enhancement in the signal can be observed until 60 min when the signal becomes saturated. However, 45 min of incubation is considered as the optimum incubation time to minimise the time consumption.

Electrochemical competitive aptasensor

The optimised assay was applied for the determination of ZEA in solutions of increasing ZEA concentrations from 0.001 to 1000 ng·mL^{-1}. The competition was done between the immobilised ZEA on the gold electrode and the free ZEA in the solution for a fixed amount of the aptamer added to each sample (50 nM). The electrochemical determination was performed using SWV technique, and the signal was analysed based on the $(i_0\text{-}i)/i_0\%$ signal. SWV can be considered as one of the most sensitive electrochemical methods used to evaluate the analytical routine of electrochemical sensors. The electrochemical determination was measured based on the electron transfer of $[Fe(CN)_6]^{4-/3-}$ redox pair onto the electrode. As shown in Fig. 5a, with increasing the concentration of the free ZEA in the solution, the amount of the aptamer available for binding to the immobilised ZEA on the gold electrode surface was limited and subsequently caused high current response. Therefore, with higher concentration of the analyte, lower change in the sensor response, $(i_0\text{-}i)/i_0\%$ was obtained. Meanwhile, with the presence of lower concentration of free ZEA, there is abundance of aptamer to bind to the immobilised ZEA on the electrode. Hence, higher sensor response was produced due to the introduction of more negative charges to the electrode surface, originating from the phosphate groups of aptamer chain.

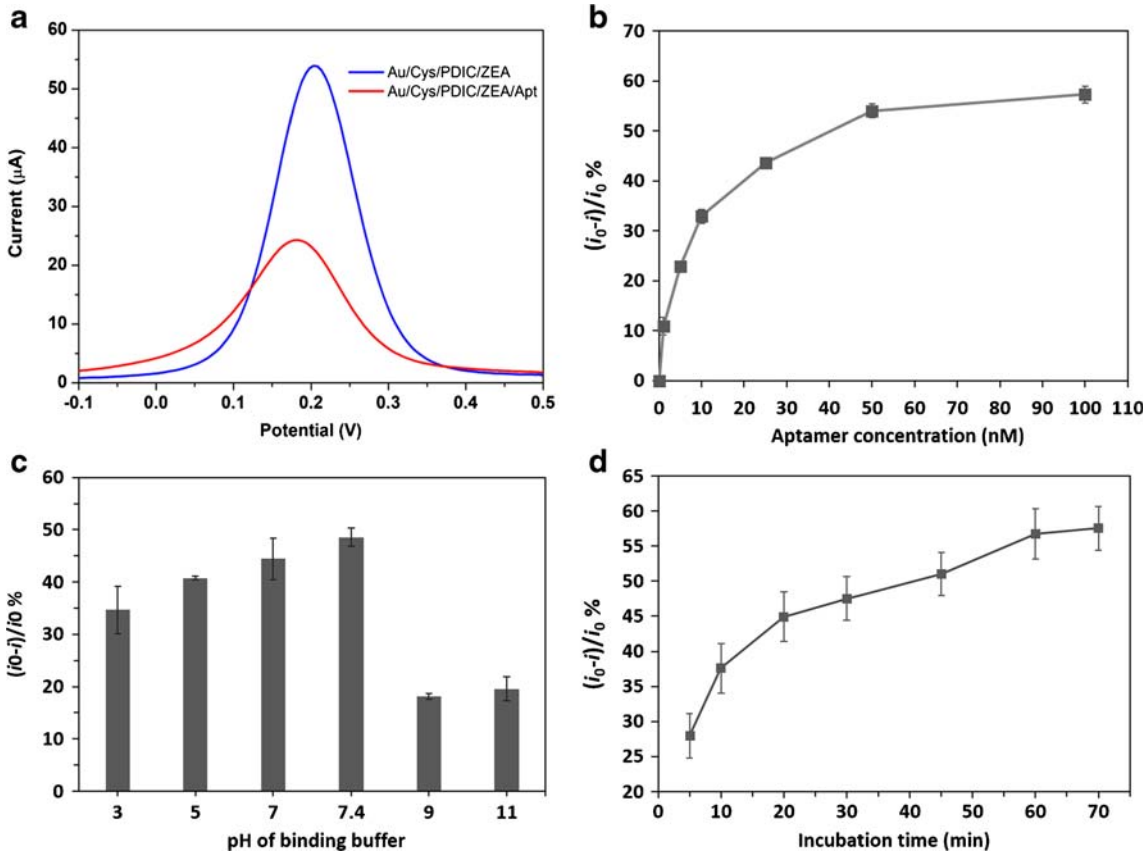

Fig. 4 **a** SWV signals of modified electrodes before (Au/Cys/PDIC/ZEA) and after incubation with the aptamer (Au/Cys/PDIC/ZEA/Apt), optimisation of: **b** aptamer concentration, **c** pH of binding buffer and **d** incubation time. The ZEA aptamer binding was observed by measuring the $(i_0\text{-}i)/i_0$% signal in 10 mM PBS containing 5 mM $[Fe(CN)_6]^{4-/3-}$ redox couple after incubation the ZEA modified electrode with ZEA aptamer. The error bars represent the standard deviations of the experiments

A linear calibration plot is shown in Fig. 5b by plotting the analytical response, $(i_0\text{-}i)/i_0$% signal vs. ZEA concentration. The linear plot has a negative slope which indicates that the sensor response signal is decreasing as the ZEA concentration is increasing. The calibration plot was fitted to a linear equation ($y = mx + c$), where y is the $(i_0\text{-}i)/i_0$% signal, m is the slope of the gradient and c is the y-intercept. The best-fit values of the experimental data were $y = -8.296x + 39$, with a coefficient of determination, $R^2 = 0.989$. The limit of detection (LOD) was calculated as 3 × SD of the blank/slope to be

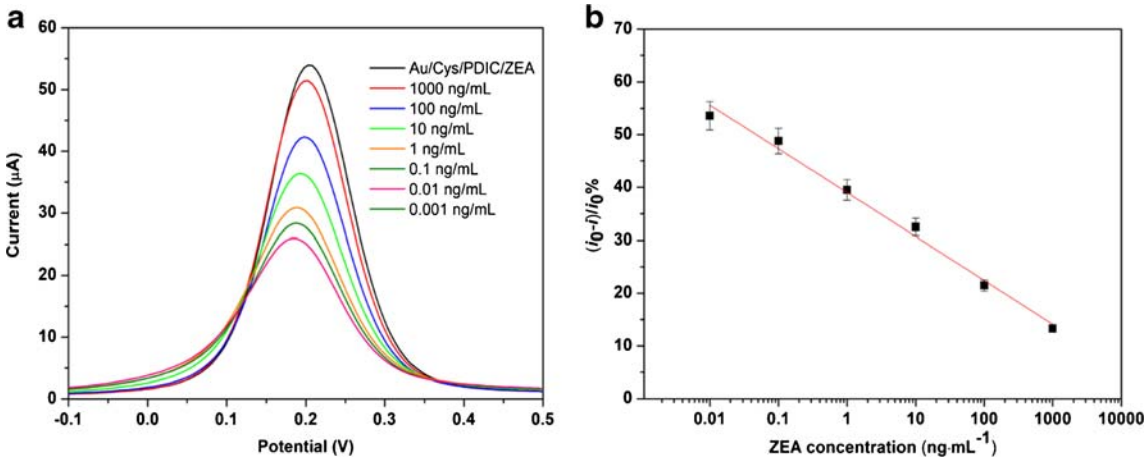

Fig. 5 **a** Competitive determination of different concentrations of ZEA using SWV technique after incubation with 50 nM aptamer, **b** linear calibration plot of the ZEA aptasensor with regression equation: $y = -8.296x + 39$, $R^2 = 0.989$. The plot represents the $(i_0\text{-}i)/i_0$% signal vs. logarithm of the ZEA concentrations (ng·mL^{-1}). The error bars show the standard deviation of two experiments

Table 1 Reported aptamer-based biosensors for the determination of ZEA in various samples

Aptamer label	Transducer	Linear range	Detection limit	Sample	Reference
Fluorescein	Fluorescence	0.5–64 ng mL^{-1}	0.5 ng mL^{-1}	Beer and wine	[22]
Magnetic nanoparticles	Fluorescence	0.05–100 μg L^{-1}	0.126 μg kg^{-1}, 0.007 μg L^{-1}	Maize, beer	[21]
Magnetic nanoparticles	Fluorescence	0.001–10 ng·mL^{-1}	0.21 pg·mL^{-1}	Maize and wheat	[20]
Thiol	Colorimetric	20–80,000 ng L^{-1}	10 ng mL^{-1}	Human serum	[24]
Label-free	Colorimetric	4–128 ng mL^{-1}	4 ng mL^{-1}	Maize powder and mouse feed	[37]
Label-free	Colorimetric	10–250 ng mL^{-1}	10 ng mL^{-1}	Maize and maize oil	[23]
Gold nanoparticles	Lateral flow	5–200 ng mL^{-1}	20 ng mL^{-1}	Maize	[25]
Thiol	Electrochemical	0.0005–500 ng mL^{-1}	0.000167 ng mL^{-1}	Maize	[26]
Label-free	Electrochemical	0.01–1000 ng mL^{-1}	0.017 ng mL^{-1}	Grain maize	This work

0.017 ng·mL^{-1}. To compare the performance of this electrochemical aptasensor with other aptasensors, Table 1 summarised various reported aptamer-based aptasensors for the determination of ZEA. The results show good sensitivity compared with other methods.

Analysis of ZEA in maize grain sample

To further study the practicability of the aptasensor for real sample applications, determination of ZEA in maize grain sample was carried out. As shown in Table 2, a good recovery percentage within 87 to 112% was obtained for determination of ZEA in the maize grain sample extract. The spiked extract was diluted to tenfold in order to reduce the food matrix effect. Hence, the results confirm the possible application of the aptasensor in real sample analysis.

Cross-reactivity study of the ZEA aptasensor

The selectivity and reliability of the sensing system of the aptasensor towards ZEA were evaluated by performing the cross-reactivity experiments using the analogues of ZEA including α-ZEL, β-ZEL and ZEA-14-Glc, as well as other types of mycotoxin such as deoxynivalenol (DON) and fumonisin B1 (FB1). The competitive assay was done as described in Section 2.7. However, the free ZEA in the solution was replaced with 10 ng·mL^{-1} of each toxin. As shown in Fig. 6, the aptasensor signal was comparable for the ZEA and the other three analogues (α-ZEL, β-ZEL and ZEA-14-glc). This indicates high degree of cross-reactivity occurs within the compounds which have similar structures. High degrees of cross-reactivity of the aptamers to similar analogues of small molecules are commonly observed such as brevetoxin-2 (BTX-2) and brevetoxin-3 (BTX-3) [27]. Luan et al. have also reported that the ochratoxin B (OTB) and ochratoxin A (OTA) possess similar binding ability towards the OTA aptamer [38]. It is believed that this cross-reactivity could be an advantage for total zearalenone determination. High signal change can be observed with the other mycotoxins which have totally different structures from zearalenone. This indicates high selectivity of the aptamer.

Table 2 Recoveries of ZEA at different concentrations of spiked maize grain sample for applicability of aptamer assay in real matrix ($n = 3$)

Spike ZEA (ng/mL)	Detected ZEA (ng/mL)	Recoveries (%)
0.0	0.01 ± 0.89	–
0.1	0.13 ± 0.02	110.0
1.0	0.89 ± 0.06	87.3
10.0	9.58 ± 0.69	95.7

Conclusion

The study has demonstrated a simple and label-free aptamer-based biosensor for the determination of ZEA based on competitive format. Truncated ZEA aptamer was successfully applied as the biorecognition molecule to determine the presence of ZEA with high affinity. The aptasensor showed good selec-

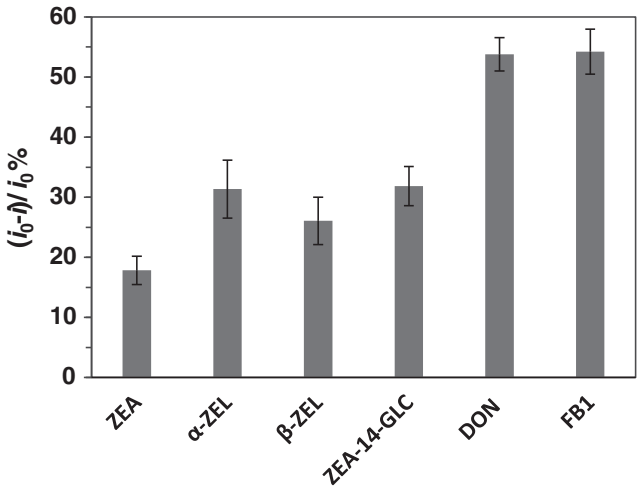

Fig. 6 Cross-reactivity study of the ZEA aptasensor and comparison of response towards α-ZEL, β-ZEL, ZEA-14-Glc, DON and FB1

tivity and sensitivity to ZEA. Although high degree of cross-reactivity between the three similar analogues of ZEA can be observed, the results demonstrated that the aptasensor did not cross-react with other mycotoxins. The practical applicability of the aptasensor was also investigated by detecting ZEA in real maize grain sample, signifying a promising feature for the analytical application in complex food samples. In view of these advantages, the method shows great potential for mycotoxin determination applications. However, the need of the washing step and the immobilization of the analyte on the electrode surface are limitations for the competitive assay. Therefore, further study needs to be done to develop a portable determination method and aptasensor based on direct assay. Several different truncation series of the aptamer will be studied in the future to determine which part among the full aptamer sequence is crucial for the binding and can be beneficial for further application in various type of sensor development.

Funding information This work was kindly supported by the Ministry of Education Malaysia through the Higher Institution Centre of Excellence (HICoE) grant scheme – project no. HICoE-ITAFoS/2017/FS6/6369114 and special appreciation to Universiti Putra Malaysia for providing Graduate Research Fellowship (GRF) to the first author. The author would also like to thank Biosensors BioMEMS and Bionanotechnology Laboratory (BBBL), Alfaisal University for providing the chemicals and instrumentations throughout this work.

Compliance with ethical standards

Conflict of interest The authors declare that they have no conflict of interest.

References

1. Choudhary AK, Kumari P (2010) Management of mycotoxin contamination in preharvest and postharvest crops: present status and future prospect. J Phytol 2:37–52
2. Richard JL (2007) Some major mycotoxins and their mycotoxicoses-an overview. Int J Food Microbiol 119:3–10
3. Leffers H, Næsby M, Vendelbo B, Skakkebæk NE, Jørgensen M (2001) Oestrogenic potencies of zeranol, oestradiol, diethylstilboestrol, Bisphenol-a and genistein: implications for exposure assessment of potential endocrine disrupters. Hum Reprod 16:1037–1045
4. Mitterbauer R, Weindorfer H, Safaie N, Krska R, Lemmens M, Ruckenbauer P, Kuchler K, Adam G (2003) A sensitive and inexpensive yeast bioassay for the mycotoxin zearalenone and other compounds with estrogenic activity. Appl Environ Microbiol 69: 805–811
5. De Saeger S, Sibanda L, Van Peteghem C (2003) Analysis of zearalenone and α-zearalenol in animal feed using high-performance liquid chromatography. Anal Chim Acta 487:137–143
6. Nuryono N, Noviandi CT, Böhm J, Razzazi-Fazeli E (2005) A limited survey of zearalenone in Indonesian maize-based food and feed by ELISA and high performance liquid chromatography. Food Control 16:65–71
7. Wang YK, Zou Q, Sun JH, Wang HA, Sun X, Chen ZF, Yan YX (2015) Screening of single-stranded DNA (ssDNA) aptamers against a zearalenone monoclonal antibody and development of a ssDNA-based enzyme-linked oligonucleotide assay for determination of zearalenone in corn. J Agric Food Chem 63:136–141
8. He QH, Xu Y, Wang D, Kang M, Huang ZB, Li YP (2012) Simultaneous multiresidue determination of mycotoxins in cereal samples by polyvinylidene fluoride membrane based dot immunoassay. Food Chem 134:507–512
9. Chauhan R, Singh J, Sachdev T, Basu T, Malhotra BD (2016) Recent advances in mycotoxins detection. Biosens Bioelectron 81:532–545
10. Radi AE, Eissa A, Wahdan T (2019) Voltammetric behavior of mycotoxin zearalenone at a single walled carbon nanotube screen-printed electrode. Anal Methods 11:4494–4500
11. Foubert A, Beloglazova NV, Hedström M, De Saeger S (2019) Antibody immobilization strategy for the development of a capacitive immunosensor detecting zearalenone. Talanta 191:202–208
12. Liu N, Nie D, Tan Y, Zhao Z, Liao Y, Wang H, Sun C, Wu A (2017) An ultrasensitive amperometric immunosensor for zearalenones based on oriented antibody immobilization on a glassy carbon electrode modified with MWCNTs and AuPt nanoparticles. Microchim Acta 184:147–153
13. Riberi WI, Tarditto LV, Zon MA, Arévalo FJ, Fernández H (2018) Development of an electrochemical immunosensor to determine zearalenone in maize using carbon screen printed electrodes modified with multi-walled carbon nanotubes/polyethyleneimine dispersions. Sensors Actuators B Chem 254:1271–1277
14. Goud KY, Kumar VS, Hayat A, Gobi KV, Song H, Kim KH, Marty JL (2019) A highly sensitive electrochemical immunosensor for zearalenone using screen-printed disposable electrodes. J Electroanal Chem 832:336–342
15. Chen X, Huang Y, Duan N, Wu S, Ma X, Xia Y, Zhu C, Jiang Y, Wang Z (2013) Selection and identification of ssDNA aptamers recognizing zearalenone. Anal Bioanal Chem 405:6573–6581
16. Ruscito A, DeRosa MC (2016) Small-molecule binding aptamers: selection strategies, characterization, and applications. Front Chem 4:1–14
17. Darmostuk M, Rimpelova S, Gbelcova H, Ruml T (2015) Current approaches in SELEX: an update to aptamer selection technology. Biotechnol Adv 33:1141–1161
18. Scheller F, Yarman A, Bachmann T, Hirsch T, Kubick S, Renneberg R, Schumacher S, Wollenberger U, Teller C, Bier FF (2013) Future of biosensors: a personal view. In: Gu MB, Kim H-S (eds) Biosensors based on aptamers and enzymes. Springer, Berlin Heidelberg, Heidelberg, pp 1–28
19. Famulok M, Mayer G (2014) Aptamers and SELEX in chemistry & biology. Chem Biol 21:1055–1058
20. Niazi S, Wang X, Pasha I, Khan IM, Zhao S, Shoaib M, Wu S, Wang Z (2018) A novel bioassay based on aptamer-functionalized magnetic nanoparticle for the detection of zearalenone using time resolved-fluorescence NaYF4:Ce/Tb nanoparticles as signal probe. Talanta 186:97–103
21. Wu Z, Xu E, Chughtai MFJ et al (2017) Highly sensitive fluorescence sensing of zearalenone using a novel aptasensor based on upconverting nanoparticles. Food Chem 230:673–680
22. Yugender Goud K, Hayat A, Satyanarayana M, Kumar VS, Catanante G, Gobi KV, Marty JL (2017) Aptamer-based zearalenone assay based on the use of a fluorescein label and a functional graphene oxide as a quencher. Microchim Acta 184: 4401–4408
23. Sun S, Zhao R, Feng S, Xie Y (2018) Colorimetric zearalenone assay based on the use of an aptamer and of gold nanoparticles with peroxidase-like activity. Microchim Acta 185:1–7
24. Taghdisi SM, Danesh NM, Ramezani M, Emrani AS, Abnous K (2018) Novel colorimetric aptasensor for zearalenone detection based on nontarget-induced aptamer walker, gold nanoparticles, and exonuclease-assisted recycling amplification. ACS Appl Mater Interfaces 10:12504–12509

25. Wu S, Liu L, Duan N, Li Q, Zhou Y, Wang Z (2018) Aptamer-based lateral flow test strip for rapid detection of zearalenone in corn samples. J Agric Food Chem 66:1949–1954
26. He B, Yan X (2019) An amperometric zearalenone aptasensor based on signal amplification by using a composite prepared from porous platinum nanotubes , gold nanoparticles and thionine-labelled graphene oxide. Microchim Acta 186:383–392
27. Eissa S, Siaj M, Zourob M (2015) Aptamer-based competitive electrochemical biosensor for brevetoxin-2. Biosens Bioelectron 69: 148–154
28. Shim W, Jin M, Mun H, Kim M (2014) An aptamer-based dipstick assay for the rapid and simple detection of aflatoxin B1. Biosens Bioelectron 62:288–294
29. Tlili C, Sokullu E, Safavieh M, Tolba M, Ahmed MU, Zourob M (2013) Bacteria screening, viability, and confirmation assays using bacteriophage-impedimetric/loop-mediated isothermal amplification dual-response biosensors. Anal Chem 85:4893–4901
30. Ghoreishi SM, Behpour M, Khoobi A, Salavati-Niasari M (2013) Electrochemical study of a self-assembled monolayer of N,N′-bis[(E)-(1-pyridyl)methylidene]-1,3-propanediamine formed on glassy carbon electrode: Preparation, characterization and application. Anal Methods 5:6727–6733
31. Gajêcka M, Zielonka U, Browski MD, Gajêcki M (2011) Threats resulting from the presence of zearalenone in water *. Med Wer 67: 643–646
32. Ganesh V, Muthurasu A (2012) Strategies for an enzyme immobilization on electrodes: structural and electrochemical characterizations. J Phys Conf Ser 358
33. Blind M, Blank M (2015) Aptamer selection technology and recent advances. Mol Ther - Nucleic Acids 4:e223
34. Le TT, Chumphukam O, Cass AEG (2014) Determination of minimal sequence for binding of an aptamer. A comparison of truncation and hybridization inhibition methods. RSC Adv 4:47227–47233
35. Stoltenburg R, Reinemann C, Strehlitz B (2007) SELEX-A (r)evolutionary method to generate high-affinity nucleic acid ligands. Biomol Eng 24:381–403
36. Cai S, Yan J, Xiong H, Liu Y, Peng D, Liu Z (2018) Investigations on the interface of nucleic acid aptamers and binding targets. Analyst 143:5317–5338
37. Zhang Y, Lu T, Wang Y, Diao C, Zhou Y, Zhao L, Chen H (2018) Selection of a DNA aptamer against zearalenone and docking analysis for highly sensitive rapid visual detection with label-free aptasensor. J Agric Food Chem 66:12102–12110
38. Luan Y, Chen J, Li C, Xie G, Fu H, Ma Z, Lu A (2015) Highly sensitive colorimetric detection of ochratoxin a by a label-free aptamer and gold nanoparticles. Toxins (Basel) 7:5377–5385